Supported ionic liquids as customizable materials to purify immunoglobulin G

Emanuel V. Capela [a], Jéssica Bairos [a], Augusto Q. Pedro [a], Márcia C. Neves [a], M. Raquel Aires-Barros [b], Ana M. Azevedo [b], João A.P. Coutinho [a,*], Ana P.M. Tavares [a], Mara G. Freire [a,*]

[a] CICECO – Aveiro Institute of Materials, Department of Chemistry, University of Aveiro, 3810-193 Aveiro, Portugal
[b] IBB – Institute for Bioengineering and Biosciences, Department of Bioengineering, Instituto Superior Técnico, Universidade de Lisboa, Av. Rovisco Pais, 1049-001 Lisbon, Portugal

A B S T R A C T

Over the past few years, antibodies such as immunoglobulin G, IgG, have increased their market share as alternative therapeutics. However, their production at high purity levels is still costly due to the absence of a cost-effective platform for their recovery and purification from the complex biological media in which they are produced. This work describes, for the first time, that materials modified with ionic liquids (ILs) can be designed for the effective capture and purification of antibodies from complex matrices, allowing both the selective adsorption of IgG or the selective adsorption of other proteins present in the media. The best results correspond to IgG with 59 % of yield and 84 % of purity in the aqueous solution, and IgG with 76 % of yield and 100 % of purity on the surface of one SIL due to the selective adsorption of IgG from human serum. The best conditions and materials were then applied to other IgG-containing matrices, namely rabbit serum and Chinese hamster ovary (CHO) cell culture supernatants, proving the robustness of the developed strategy. Furthermore, it is demonstrated that the secondary structure of IgG is preserved during the purification process and that these antibodies remain biologically active. In summary, it is shown that by only changing the IL chemical structure at the material surface it is possible to selectively adsorb IgG or to adsorb other proteins leaving IgG in solution. These findings prove that SILs are customizable materials with future potential to act in the flow-through or bind-and-elute modes. Therefore, SILs can be envisioned as potential chromatographic columns capable of substituting the high-cost commercial chromatographic columns based on biological ligands currently used to purify IgG.

1. Introduction

In a time where the efficacy of conventional drugs is declining and population is aging, the biopharmaceuticals market is currently-one of the fastest growing segments of the pharmaceutical industry [1]. In recent decades, biopharmaceuticals have proven their high specificity, low risk and low adverse effects to the patients [2]. In this context, therapies based on polyclonal (pAbs) and monoclonal (mAbs) antibodies have emerged. Plasma-derived human IgGs are increasingly used for the treatment of genetic and acquired immunodeficiencies and for several inflammatory and autoimmune disorders [3,4]. Regarding mAbs, they present a high potential for different applications, such as immunotherapy and for the treatment of cancer, transplant rejection, inflammatory and autoimmune diseases [5]. In order to be used in these applications, antibodies must meet standards of safety, efficacy, potency and purity [5].

Several advances were achieved in the past years regarding the upstream processing of antibodies increasing its productivity; however, improvements in the downstream processing have been ignored since the biopharmaceuticals industries are unwilling to replace well-established processes [6]. The downstream processing is now considered the bottleneck in antibodies production, accounting for up to 80 % of the total production costs [7]. The traditional downstream scheme used by the biopharmaceutical industry usually includes multiple steps for the recovery, isolation, purification and polishing, including several chromatographic operations for the selective capture and purification steps [8]. The affinity chromatography using protein A (proA) that is an affinity biological ligand, is the "gold standard" of the pharmaceutical

industry for the capture and purification of antibodies, representing the largest fraction of the costs of the chromatographic steps.

Besides non-chromatographic methods that could be valuable alternatives for the downstream processing of antibodies [9], several chromatographic platforms have been proposed during the last years, including cation exchange chromatography [10,11], anion exchange chromatography [12], hydrophobic interaction chromatography [13], multimodal chromatography [14], immobilized metal affinity chromatography [15], expanded bed adsorption chromatography [16], continuous annular chromatography [17] and affinity chromatography [18,19]. In addition, mimetic resins can also be considered as potential alternatives to proA chromatography, for instance matrices that specifically bind IgG such as protein G and L, synthetic ligands, proA-like porous polymeric monoliths or bioengineered peptides [20–23], in which the contributions by Roque and collaborators are significant [24–26]. Nevertheless, the development of simpler and cost-efficient techniques capable to separate, extract and purify antibodies and other proteins of relevance is still an open field.

Supported ionic liquids (SILs) are a class of materials with potential to be employed in the capture/purification of proteins [27–30]. The main advantage of ionic liquids (ILs) in the field of separation is their capacity to be designed, i.e., the possibility of manipulating their cation and anion structures to obtain the desired properties and thus improve separation performance and selectivity of a target compound such as proteins [31]. This important property is also featured in SILs, since ILs are the functional groups of a matrix (to which they are covalently bound), allowing different interactions to be established between the target compounds and the solid support, ultimately leading to increased selectivity when processing complex biological matrices. Most SILs investigated up to date have been applied as enzymatic supports [32] or in the capture of gases [33]. In addition to these applications, SILs have been reported for the separation of various molecules, such as inorganic/organic anions [34–36], metals [30,37,38] and small organic molecules [39,40]. Despite their relevance in bioprocessing, few works have been reported in the extraction/separation of biomolecules, such as proteins [41–43]. Shu et al. [41] reported an ionic liquid–polyvinyl chloride based on *N*-methylimidazole capable to successfully adsorb lysozyme, cytochrome *c* and haemoglobin, with yields of 97 %, 98 % and 94 %, respectively, while the adsorption capacity for acidic proteins such as IgG, bovine serum albumin (BSA) and transferrin was negligible. All these studies were carried out with model protein solutions. Even though the material was finally applied to the extraction of haemoglobin from human whole blood, the authors did not provide the purity levels obtained [41]. In the same line, Zhao et al. [42] successfully demonstrated the use of imidazolium-modified polystyrene (*N*-methylimidazole and crosslinked chloromethyl polystyrene resin) for the extraction of cytochrome *c* from horse heart and bovine haemoglobin with yields of 93 % and 91 %, respectively, while the retention of other proteins (IgG, BSA and transferrin) was negligible. Also, the material was applied to the extraction of haemoglobin from human whole blood; however, no purity levels were provided [42]. More recently, Song et al. [43] used an imidazolium hydrogen sulfate modified silica gel for the extraction/purification of BSA from cow's blood, achieving 28 % of yield and a purity of 91 %. The mentioned works highlight the potential of SILs to recover proteins [41–43]. Nevertheless, only one work [43] gives indication regarding the selectivity/performance of the studied materials when applied to real and complex matrices, in which a large number of proteins and other metabolites are present.

Despite the success of SILs in the processing of biomolecules, to the best of our knowledge, they were not previously applied for the purification of antibodies. In this work, a silica matrix was functionalized with three ILs, the materials were chemically, surface and morphologically characterized, and finally evaluated as adsorbents for the capture and purification of human antibodies from serum samples. The process was optimized in terms of solid:liquid ratio, pH and contact time in order to develop cost-effective strategies. Finally, the best conditions were applied to other IgG-containing matrices (rabbit serum and Chinese hamster ovary (CHO) cell culture supernatants) to demonstrate the applicability of the developed SIL-based platforms to bioprocess other matrices.

2. Materials and methods

The chemicals used for the activation of silica (used as supporting material) were silica gel (60 Å) with a particle size of 0.2–0.5 mm from Merck and hydrochloric acid (HCl, purity 37 wt%) from Sigma-Aldrich. The solvents used to prepare the IL-functionalized silica were toluene (99.98 % purity) and ethanol (99.99 % purity) both from Fisher Scientific; methanol (99.99 % purity) from Fisher Chemical; (3-chloropropyl) trimethoxysilane (98 % purity), *N*-methylimidazole (99 % purity), tributylamine (99 % purity) provided by Acros Organics; and trioctylamine (>98 % purity) acquired from Fluka.

For the HPLC mobile phase, the following salts were used: anhydrous monobasic sodium phosphate (99–100.5 % purity), sodium phosphate dibasic heptahydrate (98–102 % purity), and sodium chloride (99.5 % purity), all provided by Panreac.

The biologicals used in this work were human IgG for therapeutic administration (trade name: Gammanorm®), obtained from Octapharma (Lachen, Switzerland), as a 165 mg.mL^{-1} solution; HSA (96 % purity) provided by Alfa Aesar; human serum from human male AB plasma, USA origin, sterile-filtered, obtained from Sigma-Aldrich (H4522 Sigma) (≥95.0 % purity); rabbit serum (containing 0.01 % of thimerosal) unconjugated and pooled from a normal donor population, also purchased from Sigma-Aldrich. The CHO cell culture supernatant containing anti-human interleukin-8 (anti-IL-8) monoclonal antibodies (mAbs) was produced in-house according to the details presented in the Supplementary Material. The produced anti-IL-8 mAb has an isoelectric point (pI) of 9.3 [44]. The Quantikine® Human IL-8/CXCL8 kit (R&D systems, Minneapolis, MN, USA) was used for competitive enzyme linked immunosorbent assay (ELISA) experiments.

In order to investigate the effect of pH on the adsorption behaviour of IgG and albumin, distinct buffer solutions were used: phosphate buffered saline (PBS) tablets was acquired from Sigma-Aldrich-Merck KGaA (St Louis, Missouri, USA). One tablet of PBS was dissolved in 200 mL of distilled water yielding 0.01 M phosphate buffer, 0.0027 M potassium chloride and 0.137 M sodium chloride, pH 7.4, at 25 °C. From pH 3 to pH 7: citrate/phosphate buffer (0.1 M citric acid/0.2 M Na$_2$HPO$_4$); from pH 9 to pH 11: carbonate-Bicarbonate buffer: (0.1 M Na$_2$CO$_3$/0.1 M NaHCO$_3$); pH 12: Glycine-NaOH buffer (0.1 M glycine + 0.1 M NaCl/0.1 M NaOH).

Other reagents used in this work were of analytical grade and used as acquired, without further purification steps.

2.1. Synthesis of SIL materials

Three different SIL materials were herein synthesized, namely a 1-methyl-3-propylimidazolium-based supported silica with chloride as the counter ion ([Si][C$_3$mim]Cl), a propyltributylammonium-based supported silica with chloride as the counter ion ([Si][N$_{3444}$]Cl) and a propyltrioctylammonium-based supported silica with chloride as the counter ion ([Si][N$_{3888}$]Cl). The synthesis of SILs was adapted from the method described by Qiu et al. [35], and previously proposed by us [39,40,45]. The initial step for the synthesis of the SIL materials consists in the activation of the silica gel (pore size of 60 Å) with a solution of hydrochloric acid (37 wt%) for 24 h to increase the content of silanol groups on the silica surface. Subsequently, the activated silica was washed with *ca.* 2 L of distilled water, until the washing water achieves the distilled water pH, and then placed in the kiln for 24 h at 60 °C. In the next step the activated silica was functionalized with 3-chloropropyltrimethoxysilane. For that 5.0 g of activated silica was suspended in 60 mL of toluene and 5.0 mL (0.026 mol) of 3-chloropropyltrimethoxysilane added. Then, the mixture was refluxed under magnetic stirring (550

rpm) for 24 h at 115 °C to obtain the intermediate material 3-chloropropylsilane ([Si][C$_3$]Cl). Afterwards, the obtained material was filtered and washed with 100 mL of toluene, 200 mL of 1:1 mixture of ethanol: water, 500 mL of distilled water and 100 mL of methanol, and finally dried for 24 h at 60 °C. The third step in the SILs synthesis consisted in the functionalization of the [Si][C$_3$]Cl, by mixing 5.0 g of the material with 50 mL of toluene and 5 mL of the respective cation source (*N*-methylimidazole, tributylamine or trioctylamine; *cf.* Fig. 1). Thus, the chemical amount of the cation source was 0.061, 0.021 and 0.011 mol respectively. The suspension was magnetically stirred under reflux for 24 h. Finally, the obtained materials were filtered and washed with 100 mL of toluene, 350 mL of methanol, 300 mL of distilled water and 150 mL of methanol, and once again dried for 24 h at 60 °C. In Fig. 1, a schematic representation of the synthesis protocol used for the preparation of the SILs under study is provided.

2.2. Characterization of SILs materials

The synthesized materials were characterized through several techniques, namely elemental analysis, solid-state ^{13}C nuclear magnetic resonance (NMR) spectroscopy, attenuated total reflectance Fourier-transform infrared (ATR-FTIR) spectroscopy, point zero charge (PZC), and scanning electron microscopy (SEM).

The content of carbon, hydrogen and nitrogen of the three SILs ([Si][C$_3$mim]Cl, [Si][N$_{3444}$]Cl and [Si][N$_{3888}$]Cl) were determined by elemental analysis technique using the TruSpec LECO-CHNS 630–200-200 analyser. A small amount of solid sample (~2 mg) was placed and analysed at a combustion furnace temperature of 1075 °C and an afterburner temperature of 850 °C. Infrared absorption was used to determine the carbon and hydrogen contents whereas thermal conductivity was used for nitrogen quantification.

Solid-state carbon-13 Nuclear Magnetic Resonance (^{13}C NMR)
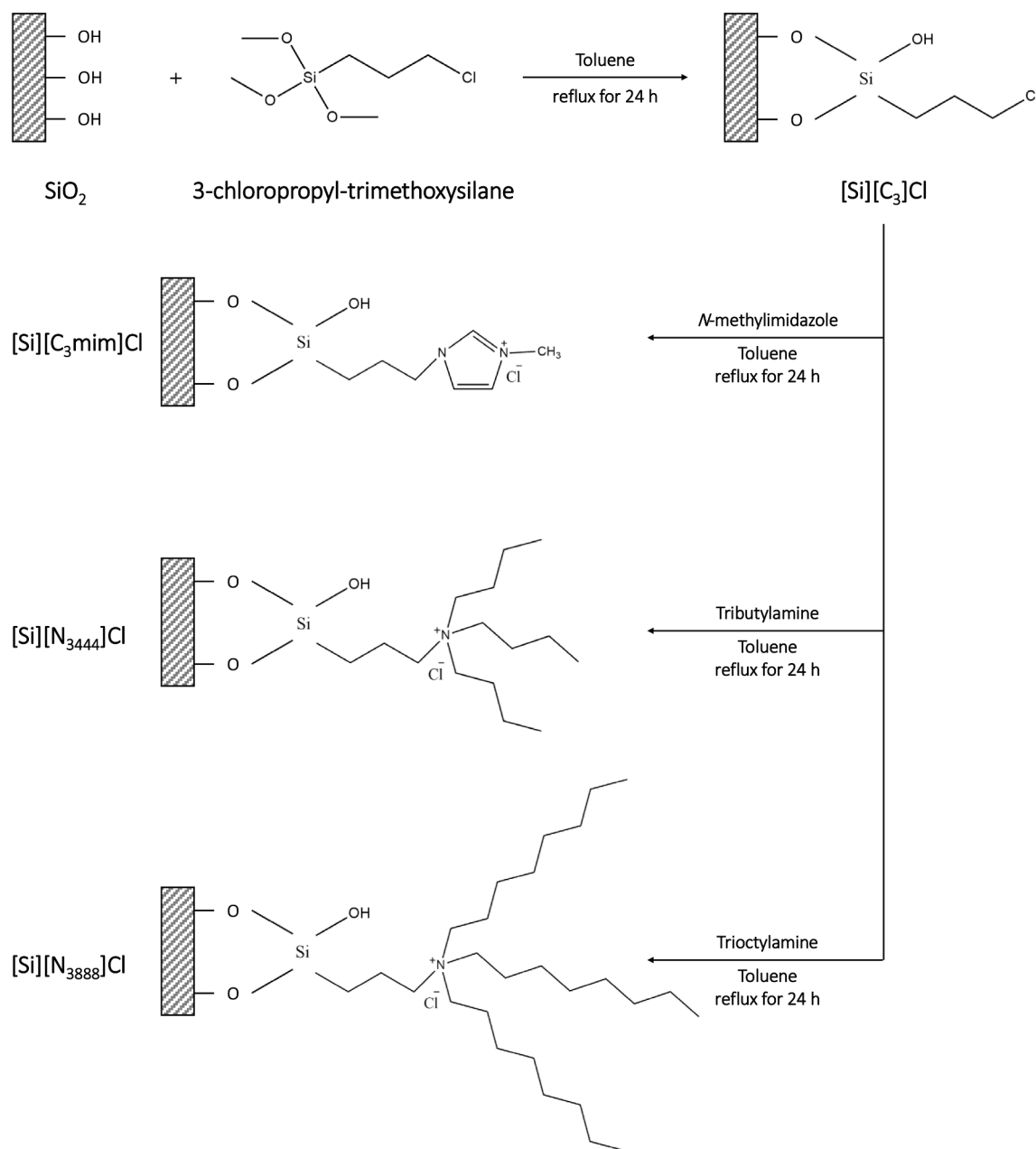

Fig. 1. Schematic representation of the preparation of SILs, their chemical structures and respective abbreviations – [Si][C$_3$mim]Cl, [Si][N$_{3444}$]Cl and [Si][N$_{3888}$]Cl. 3-chloropropylsilane ([Si][C$_3$]Cl), the intermediate of the two-step reaction, is also represented.

spectroscopy was used to confirm the SILs preparation. The spectra of the three SIL materials were recorded at 9.4 T, on a spectrometer BRUKER AVANCE III (wide-bore). A 4 mm double-resonance MAS probe was employed at 100.6 MHz. Fourier-Transform infrared spectroscopy (FTIR) of synthesized SILs was carried out using a Perkin Elmer FT-IRSystem Spectrum BX), between 4000 and 400 cm^{-1} at a resolution of 2 cm^{-1} and 256 scans per sample. The point of zero charge (PZC) was determined by zeta potential curves. Zeta potential values were recorded for suspensions of materials in water at different pH values, which were adjusted with NaOH (0.01 M) and HCl (0.01 M) solutions, and employing a suitable cell for this purpose using a Malvern Zetasizer Nano ZS equipment (Malvern Instruments ltd. Malvern). The surface area (S_{BET}) of SiO_2 was estimated by N_2 isotherm adsorption measurements and the Brunauer-Emmett-Teller (BET) method, operating a Gemini V2.0 surface analyser from Micromeritics Instrument Corp. Prior to BET measurements, the sample was degassed at -80 °C under nitrogen flow overnight. Scanning electron microscopy (SEM) was performed using a FE-SEM Hitachi SU-70. The SILs materials were deposited on an aluminium sample holder followed by carbon coating.

2.3. Bonding amount

The chemical amount of IL per area of material, designated by bonding amount (BA) (μmol m^{-2}), was determined for [Si][C$_3$]Cl and for the synthetized SILs. Considering the S_{BET} of silica as 435 $m^2.g^{-1}$, the BA value was calculated according to Eqs. (S1-S3) given in the Supplementary Material.

2.4. Determination of the SIL-based process performance

IgG and protein impurities were quantified in all feeds and in each sample by size-exclusion high-performance liquid chromatography (SE-HPLC). Samples were diluted at a 1:2 (v:v) ratio in an aqueous potassium phosphate buffer solution (50 mmol•L^{-1}, pH 7.0, with NaCl 0.3 mol..L^{-1}) used as the mobile phase. The equipment used was a Chromaster HPLC system (VWR Hitachi) equipped with a binary pump, column oven (operating at 40 °C), temperature controlled auto-sampler (operating at 10 °C), DAD detector and a column Shodex Protein KW-802.5 (8 mm × 300 mm). The mobile phase was run isocratically with a flow rate of 0.5 mL.min^{-1} and the injection volume was 25 μL. The wavelength was set at 280 nm. The IgG calibration curve (presented in the Supplementary Material, Fig. S1) was established with commercial human IgG, with a concentration ranging from 5 to 200 mg.L^{-1}.

The process performance was evaluated by the recovery yield and purity level for IgG. In addition, both the IgG concentration and aggregation percentage were determined for a full characterization of the process outputs. The importance of evaluating the percentage of IgG aggregates is due to its biological activity since the presence of IgG aggregates compromise the therapeutic effectiveness and safety [46]. For each sample, the peaks areas were estimated using PeakFit® software, and the remaining data was treated on Excel.

The recovery yield (%Yield$_{IgG}$) of IgG, the percentage purity level of IgG (%Purity$_{IgG}$) and the aggregation percentage of IgG (%Aggregation$_{IgG}$) retained in the solution and adsorbed onto the material were determined by equations (S4-S9) given in the Supplementary Material. At least two individual experiments were performed to determine the average in performance parameters, as well as the respective standard deviations. To complement the SE-HPLC data and to infer on the total protein profile and integrity of IgG and HSA, sodium dodecyl sulphate polyacrylamide gel electrophoresis (SDS-PAGE) was performed, as described in the Supplementary Material.

2.5. Screening of the SIL materials for the purification of IgG from human serum

An initial screening was performed with all the synthesized materials

to purify IgG. Activated silica was used as a control for comparison purposes. Each SIL/activated silica was added to 2 mL microtubes under the following operating conditions: Solid:Liquid ratio (S:L ratio) of 100 mg.mL^{-1} (50 mg of supported material (SILs) and 500 μL of human serum 20-fold diluted in the appropriated buffer according to the selected pH); pH value of 3, 5, 7 and 9; and contact time of 60 min. The samples were stirred on a programmable rotator-mixer from PTR-30 Grant-bio. Finally, the samples were centrifuged in a VRW MICRO STAR 17 at 13000 rpm during 20 min to separate the aqueous solution from the material, that remained in the bottom of the microtube. All aqueous solutions were diluted at a 1:1 (v:v) ratio with the HPLC mobile phase, and then analysed by SE-HPLC.

2.6. Optimization of the purification process by factorial design experiments

After the first screening performed, factorial design was used to maximize human antibodies recovery and purification. A 2^k factorial planning was carried out, in which there are k factors that can contribute to a different response regarding the final IgG recovery yield or purity in just one step. The experimental data were treated according to Eqs S10-S12 provided in the Supplementary Material.

In this work, the 2^3 factorial planning was used aiming at the optimization of three independent variables (inputs), namely i) solid:liquid ratio (mg of material per mL of aqueous solution of biological media); ii) pH value; and iii) contact time (min), both for the maximization of the IgG yield or purity. The inputs were studied at three levels: the central point (zero level), factorial points (1 and -1, level one), and axial points (level α), being the 2^3 factorial planning provided in the Supplementary Material (Table S1). Based on Eq. (S11), a total of 17 experiments were performed for the development of the proposed factorial design. Also, for k = 3 and considering Eq. (S12), α adopts a value of 1.68. The range was defined according to preliminary results, and the chosen central point was 100 mg.mL^{-1} for S:L ratio, pH 5 and 60 min of contact time. The detailed list of experiments performed with the coded and uncoded coefficients is provided in the Supplementary Material (Table S2).

The results obtained were statistically analysed using Statsoft© STATISTICA 10.0 software and considering a confidence level of 95 %. Three-dimensional surface response plots were originated by changing two variables within the experimental range and maintaining the remaining factors at the central point. Each factorial planning developed used a central point experimentally obtained at least three times. The response surfaces and contour plots were also obtained using Statsoft© STATISTICA 10.0 software.

2.7. Optimization of the IgG purification processes

In order to further optimize the processes based on the information given by the design of experiments, a set of new conditions regarding the pH value and S:L ratio were considered for the IgG capture and/or purification using the three SILs under study ([Si][C$_3$mim]Cl, [Si][N$_{3444}$]Cl and [Si][N$_{3888}$]Cl). For the optimization of the process pH, a S:L ratio of 100 mg.mL^{-1} (50 mg of SILs and 500 μL of human serum 20-fold diluted in the appropriated buffer) and an intermediate contact time of 60 min were fixed, while pH values of 10, 11 and 12 were studied (values higher than the pI of the protein of interest, pI$_{IgG}$ = 9 [47]). Further optimization of the S:L ratio was performed for [Si][C$_3$mim]Cl, also using the three pH values (10, 11 and 12) and 60 min of contact time, and at two different S:L ratio – 150 and 200 mg·mL^{-1} (75 and 100 mg of material with 500 μL of human serum 20-fold diluted in the appropriated buffer, respectively). All the assays were prepared following the procedure described above.

2.8. Evaluation of the robustness of the processes

The two best conditions identified were finally investigated to prove

the robustness of the IgG downstream processes developed. The materials were set in contact with two new biological complex matrices, namely rabbit serum and CHO cell culture supernatants. For [Si][C$_3$mim]Cl, the operating conditions were a S:L ratio of 150 mg.mL^{-1}, pH 12 and 60 min, while for [Si][N$_{3888}$]Cl the selected operating conditions were a S:L ratio of 100 mg.mL^{-1}, pH 11 and 60 min. The experimental procedure adopted followed the one mentioned above.

2.9. Assessment of IgG stability and anti-IL-8 mAbs activity

Circular dichroism (CD) was used to address the secondary structure of IgG at different pH values and after extraction from human serum under the optimized conditions. Competitive ELISA was performed for the CHO cell culture supernatant and purified fractions from [Si][C$_3$mim]Cl to evaluate the activity of anti-human IL-8 mAbs. The mouse anti-human CXCL8/IL8 antibody (RayBiotech Life, Peachtree Corners, GA, USA) was used as positive control. Detailed information can be found in the Supplementary Material.

3. Results and discussion

3.1. Synthesis and characterization of SIL materials

Fig. 1 presents a schematic overview of the SILs synthesis procedure adopted in this work, by which three different SILs were prepared: [Si][C$_3$mim]Cl, [Si][N$_{3444}$]Cl and [Si][N$_{3888}$]Cl. Although three different cations were investigated, chloride was kept as the counterion in all SILs, avoiding the use of more complex anions, while allowing to lower the costs of the materials and reduce their eco- and cytotoxicity [39]. All SILs were prepared by a two-step reaction process where activated silica reacts with a silane-coupling agent (3-chloropropyltrimethoxysilane) and the obtained chloropropylsilica reacts with *N*-methylimidazole or other tertiary ammines (as cation sources).

Elemental analysis was carried out to quantitatively determine the carbon, hydrogen, and nitrogen contents of the prepared SILs. Considering the S$_{BET}$ value for the used silica of 435 m^2.g^{-1}, the bonding amount was calculated for chloropropylsilica and for the synthetized SILs. Zeta potential curves as function of pH (Supplementary Material, Fig. S2) were used to determine the PZC of the materials. This information is summarized in Table 1.

The intermediate [Si][C$_3$]Cl shows the presence of carbon (C) and hydrogen (H), but as expected does not contain nitrogen (N), indicating the absence of the IL cation source. It is also possible to verify that the higher the amount of cation source used, the higher the percentage of nitrogen. This increase relates to an increase of the functionalization degree, noticeable by the increase in the bonding amount. However, there is no linear dependence between the amount of cation source and the bonding amount in the case of the imidazole and the quaternary ammonium SILs based cations. The justification for this evidence may be related to stereochemical effects. According to the elemental analysis (Table 1) the amount of 2.84, 0.15 and 0.07 (in %) of N was achieved for

the SILs [Si][C$_3$mim]Cl, [Si][N$_{3444}$]Cl and [Si][N$_{3888}$]Cl, respectively. Considering the structure of the SILs, it is possible to conclude that the mass of IL *per* mass of SIL is respectively: 161.92 mg. g, 27.77 mg.g^{-1} and 21.85 mg.g^{-1}.

The successful preparation of SILs was additionally confirmed through solid-state ^{13}C Nuclear magnetic resonance (NMR), whose spectra are shown in the Supplementary Material (Fig. S3). Concerning the intermediate [Si][C$_3$]Cl spectrum, three peaks at 10, 27 and 47 ppm are assigned to the three carbons of the propyl alkyl chain. For [Si][C$_3$mim]Cl, the presence of the six peaks was noticed: the three carbon atoms of the alkyl side chain of the aromatic ring (C2, C1 and C6) corresponds to the peaks at 10, 25 and 38 ppm, respectively. The signals between 120 and 140 ppm correspond to the aromatic carbons of the imidazolium ring (C5 and C4), respectively. The last carbon of the alkyl chain (C3) corresponds to the peak at 53 ppm. Regarding to the solid-state ^{13}C NMR, the spectra of [Si][N$_{3444}$]Cl and [Si][N$_{3888}$]Cl are similar to the spectrum of the intermediate material ([Si][C$_3$]Cl), which is due to the low functionalization degree of these materials, in agreement with the elemental analysis results and the results previously reported [39].

The attenuated total reflectance Fourier-Transform infrared spectroscopy (ATR-FTIR) spectra of activated silica, chloropropyl silica, and prepared SILs were also recorded in the range of 400 and 4000 cm^{-1}. All were obtained using silica as background, being represented in the Supplementary Material (Fig. S4). At around 3400–3900 cm^{-1} it is observed a band corresponding to Si-OH stretching, which corresponds to the first step of reaction with the 3-chloropropyltrimethoxysilane. The relatively weaker bands occurring at 2900–3200 cm^{-1} are the stretching vibrations of CH$_3$ and CH$_2$, whereas the band at 1100 cm^{-1} represents the aliphatic chain C-N from all the SILs after their reaction with the corresponding cation source. Finally, the peaks at 400–900 cm^{-1} are related with the OH bending from the first reaction of the activated silica with the anion, and to the chloride anion, also from the first reaction. Overall, ATR-FTIR results also allow to confirm the silica functionalization with ILs.

All the studied materials presented different PZC values, determined from the graphical representations of the zeta potential as function of pH (Fig. S2 in the Supplementary Material). The SILs studied showed to lead to stable suspensions in water, allowing to measure the zeta potential as function of the pH. Activated Silica presents the lowest PZC value (3.0), while all the other materials have higher PZC values, ranging from 4.1 (intermediate material, [Si][C$_3$]Cl) to 8.9 ([Si][C$_3$mim]Cl). These results suggest that the surface of [Si][C$_3$mim]Cl, [Si][N$_{3444}$]Cl and [Si][N$_{3888}$]Cl is more positively charged when compared to the activated silica and to the intermediate material, therefore confirming the successful functionalization of the synthesized SILs, since they are more positively charged due to the grafting of the IL cation to the silica surface.

Finally, SEM was used to morphologically characterize the synthesized materials. The SEM images of activated silica and the synthesized SILs are given in the Supplementary Material (Fig. S5). As seen from the SEM images, the commercial silica gel 60 used does not have a homogeneous size and morphology. Overall, no significant differences in the materials morphology are observed between the prepared SILs and the non-functionalized silica obtained from the same two step procedure but without the chemical reagents (namely the silane and the IL cation source), meaning that the intermediate step and remaining steps required for silica functionalization with ILs do not change the material morphology. Nevertheless, it should be noted that the two refluxing steps with magnetic stirring have a grinding effect on the particles, which commercially have a size between 200 and 500 μm, and which after functionalization shown sizes between 10 and 100 μm. Overall, the characterization of the prepared SILs by elemental analysis, FTIR, zeta potential, CPMAS ^{13}C NMR and SEM allowed to confirm the successful functionalization of these materials.

Table 1

Chemical amount (n(mol)) of 3-chloropropyltrimethoxysilane and of the cation source in the synthesis, elemental analysis results: weight percentages of carbon (%C), hydrogen (%H), and nitrogen (%N); bonding amount (BA) (μmol.m^{-2}); and point of zero charge (PZC) of activated silica, [Si][C$_3$]Cl and all SIL materials: [Si][C$_3$mim]Cl, [Si][N$_{3444}$]Cl, and [Si][N$_{3888}$]Cl).

SILs	n (mol)	AE			BA (μmol.m^{-2})	PZC
		C (%)	H (%)	N (%)		
Activated silica	–	–	–	–	–	3.0
[Si][C$_3$]Cl	0.026	4.64	1.39	–	2.96	4.1
[Si][C$_3$mim]Cl	0.061	8.38	2.12	2.84	2.33	8.9
[Si][N$_{3444}$]Cl	0.021	5.74	1.37	0.15	0.24	5.7
[Si][N$_{3888}$]Cl	0.011	6.90	1.34	0.07	0.12	5.8

3.2. Characterization of the biological matrices

Aqueous solutions of commercially available pure IgG, pure albumin and the complex biological matrices used in this work (human serum 20-fold diluted, rabbit serum 20-fold diluted and CHO cell culture supernatants) were analysed by SE-HPLC for the characterization of their chromatographic profiles. The results obtained are presented in the Supplementary Material Fig S6.

Under the chromatographic conditions used, pure IgG samples present 2 chromatographic peaks: one corresponding to the IgG monomer and the other to IgG aggregates, with a retention time of *ca.* 15.0 min and 13.8 min, respectively, in agreement with previous reports [48,49]. The major protein impurity in the feed is human serum albumin (HSA), with a retention time of *ca.* 16.2 min. Both rabbit serum and CHO cell culture supernatant also exhibit a similar chromatographic profile. Nevertheless, it should be highlighted that in the cell culture supernatant, the main protein impurity is BSA, whereas in the rabbit serum it corresponds to rabbit albumin.

The IgG content in the human serum samples was ascertained before each assay, and it was found that its average concentration was 470.1 ± 12.5 mg.L^{-1}, with a purity of 47.0 ± 1.6 %; in CHO cell culture supernatants it was found an average concentration of IgG of 46.0 ± 5.8 mg.L^{-1} with a purity of 19.90 ± 4.5 %; finally, for rabbit serum, the IgG average concentration was found to be 297.2 ± 22.0 mg.L^{-1}, with an average purity of 24.6 ± 0.3 %.

In this work, all the assays were initially conducted using human serum, since it is a consistent and homogenous biological complex medium containing high concentrations of antibodies, and also presenting

similar composition between samples, allowing consistent and comparable results along the work and avoiding discrepancies arising from the use of different batches. CHO cell culture supernatants and rabbit serum were then selected to evaluate the applicability of the developed IgG downstream processes for different biological matrices.

3.3. Screening of SIL materials for IgG purification

An initial screening was performed to understand the behaviour of the IgG antibodies of human serum samples in the presence of activated silica (without any functionalization) and the SIL materials under study ([Si][C$_3$mim]Cl, [Si][N$_{3444}$]Cl and [Si][N$_{3888}$]Cl). For that purpose, activated silica and SILs were placed in contact with human serum samples at different pH values (ranging from 3 to 9) to evaluate the influence of the pH in the (selective) adsorption of proteins from human serum.

The same operational conditions were applied for all materials: a S:L ratio of 100 mg.mL^{-1} and 60 min of contact time, while the pH value was changed (3, 5, 7 and 9). After the contact of the human serum sample with the materials, the chromatograms of the aqueous solutions were obtained and compared with the initial chromatogram of the human serum (before contact with the material), allowing to evaluate the ability of these materials to (selectively) adsorb proteins present in the biological complex medium. The respective chromatograms are presented in Fig. 2. At the studied pH, the SE-HPLC chromatograms clearly demonstrate that the aggregates peaks intensity of the initial biological matrices is similar. Furthermore, no precipitation was observed in all experiments.
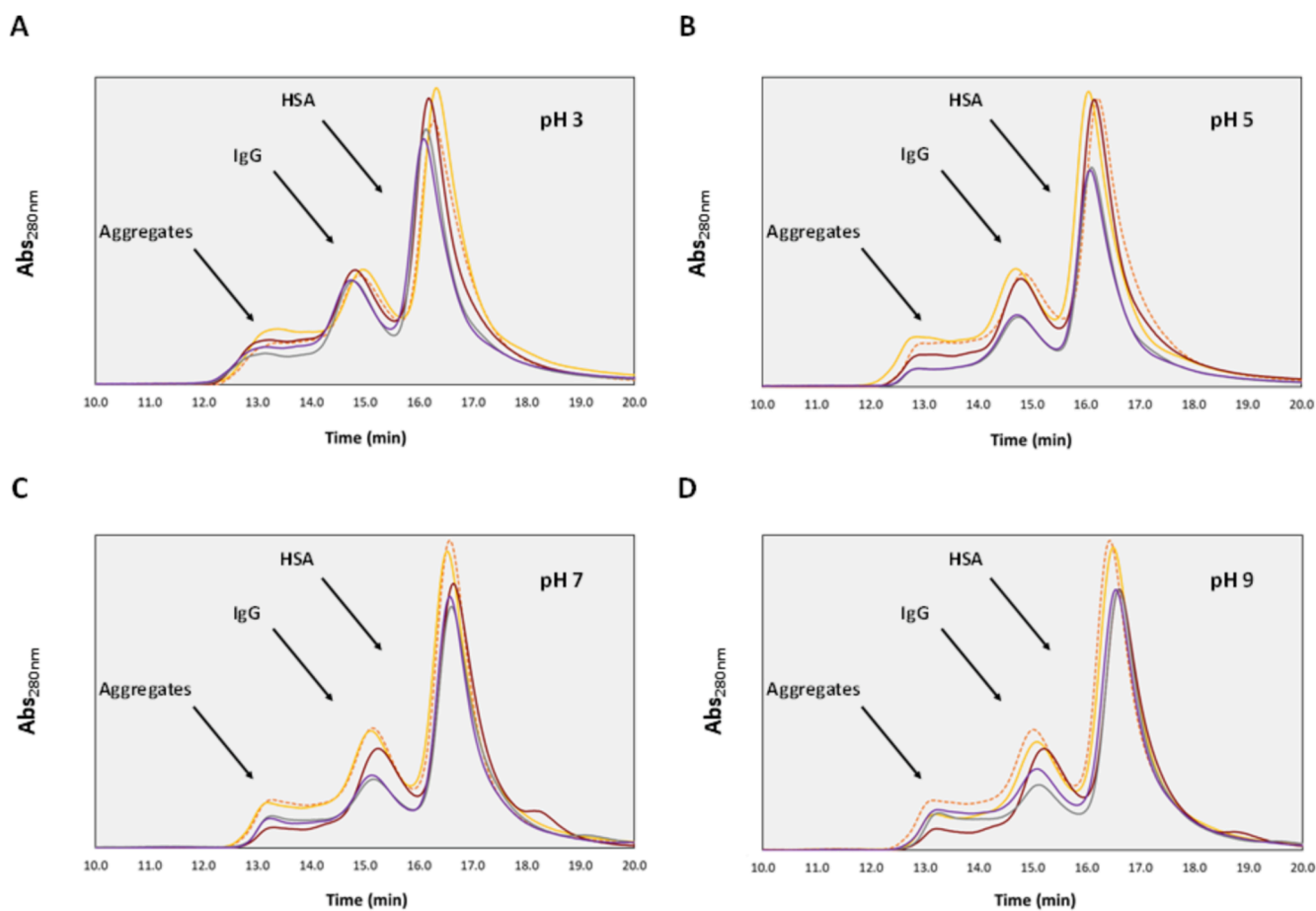

Fig. 2. SE-HPLC chromatograms of the human serum samples 20-fold diluted after contact with the supported materials under study at: (A) pH 3; (B) pH 5; (C) pH 7; and (D) pH 9. For each graph, the chromatographic profiles of human serum (•••), and human serum after contact with activated silica (–), [Si][C$_3$mim]Cl (–), [Si][N$_{3444}$]Cl (–), and [Si][N$_{3888}$]Cl (–) are presented.

Based on results provided in Fig. 2, activated silica presents no selectivity, at any of the pH values studied, and for any of the biomolecules present in human serum. In this case, similar SE-HPLC chromatograms were obtained for all aqueous solutions after contact with activated silica and the initial human serum sample. Moreover, at pH 3, similar chromatographic profiles between the initial and final samples were found for all the SILs under study, meaning that no IgG nor albumin preferentially adsorb into the materials under these conditions. This behaviour seems to be related with the fact that, at pH 3 both IgG and HSA are positively charged ($pI_{IgG} = 9.0$ and $pI_{HSA} = 4.9$). As the studied SILs are also positively charged ($PZC_{[Si][C_3mim]Cl} = 8.9$; $PZC_{[Si][N_{3444}]Cl} = 5.7$ and $PZC_{[Si][N_{3888}]Cl} = 5.8$), there is no electrostatic attraction between the proteins and the materials, preventing their adsorption.

When increasing the pH to 5, it is noticed that IgG and albumin start to adsorb into $[Si][N_{3444}]Cl$ and $[Si][N_{3888}]Cl$; however, there is no significant adsorption of proteins into $[Si][C_3mim]Cl$, since it consists in the material with most positive charges (due to the higher PZC). At pH 7, a preferential adsorption of IgG onto $[Si][N_{3444}]Cl$ and $[Si][N_{3888}]Cl$ occurs, in accordance with the pI of IgG and HSA and the PZC of the materials; both $[Si][N_{3444}]Cl$ and $[Si][N_{3888}]Cl$ are negatively charged, while IgG is positively charged. This trend reveals that electrostatic interactions may be contributing for the adsorption behaviour. However, since albumin is negatively charged and its adsorption into the materials also occurs, this means that other interactions are taking place as well. $[Si][C_3mim]Cl$ that is positively charged at the work pH, leads to the less promising results, adsorbing less IgG and albumin than the quaternary ammonium-based SILs. The adsorption of IgG (also positively charged) was unexpected, suggesting that on this material other interactions than electrostatic ones, such as hydrogen-bonding, dispersive and $\pi\ldots\pi$ interactions, play a significant role in the process.

Finally, at pH 9, both IgG and albumin were adsorbed into the three SILs, but less than at pH 7. Again the lower adsorption was observed for $[Si][C_3mim]Cl$, revealing that the pH is not a significant parameter to control the adsorption onto this SIL. Using a combination of experimental (e.g. fluorescence measurements using BSA) and computational data (molecular docking using HSA), Shu et al. [50] studied the interaction of several imidazolium-based ILs, including 1-butyl-3-methylimidazolium chloride also investigated in this work, and albumins. The authors found that at pH 7.4, electrostatic attraction between the IL cationic moieties and negatively charged BSA facilitates the binding of ILs with BSA. Additional molecular docking analysis revealed that the 1-butyl-3-methylimidazolium cation is surrounded by HSA hydrophobic residues (Phe502, Phe507, Phe509, Val547, Phe551, Leu575 and Ser579). Overall, these results suggest that hydrophobic forces may be the main interaction forces in the binding of imidazolium ILs to HSA, although electrostratic interactions might also be involved in the binding of the IL to HSA (which contains two charged amino acid residues - Lys536 and Gln580), being in good agreement with the thermodynamic analysis [50]. Generally, the interaction behaviour of HSA with the SILs synthesized in this work, particularly for $[Si][C_3mim]Cl$, are in good agreement with the results previously reported [50].

In conclusion, the data here gathered allowed to conclude that the functionalization of activated silica with ILs is fundamental to introduce selectivity in the materials (SILs); by using activated silica, no adsorption of proteins was observed in the pH range herein studied. Although for pH 3 no significant proteins adsorption could be noticed, for pH 5 it was observed a preferential IgG adsorption into two SILs, $[Si][N_{3444}]Cl$ and $[Si][N_{3888}]Cl$, whereas for $[Si][C_3mim]Cl$ it only occurs at pH 7. The higher pH values seem to favour the adsorption phenomenon as the material becomes negatively charged, as shown above. The $[Si][C_3mim]Cl$ was the SIL with the lower ability for proteins adsorption.

3.4. Optimization of the adsorption process and selectivity by factorial design experiments

Based on the most promising conditions obtained in the initial

screening of the three SILs, a 2^3 factorial planning was performed aiming at optimizing the operation conditions (S:L ratio, pH and contact time) in the SIL-based process for the capture/recovery and purification of IgG antibodies from human serum. The performance parameters ($\%Yield_{IgG}$ and $\%Purity_{IgG}$) were experimentally obtained for each assay using the three SILs. For $[Si][C_3mim]Cl$, the performance parameters were determined in the aqueous solution after contact with the supported material (since IgG is preferentially maintained in solution using this SIL), and for $[Si][N_{3444}]Cl$ and $[Si][N_{3888}]Cl$ the performance parameters refer to the material after contact with the liquid (due to the preferential adsorption of IgG onto these materials). The quantitative results obtained are presented in Table S3, while the comparison between the experimental and theoretical results, as well as the statistical analyses performed (regression coefficients and ANOVA), are presented in the Supplementary Material (Tables S4 – S21 and Figs. S6 – S11). According to the data presented in Table S3, for each SIL material there are optimal conditions providing good purity levels without impairing the IgG recovery yield (highlighted in bold).

For $[Si][C_3mim]Cl$, the IgG is completely retained in solution, i.e. 100 % of yield, with a purity of 46.9 ± 0.7 % using a S:L ratio of 50 mg. mL^{-1}, pH 3 and a contact time of 90 min. On the other hand, by using $[Si][N_{3444}]Cl$, IgG is preferentially adsorbed onto the SIL material with a yield of 57.0 ± 7.5 % and a purity level of 65.0 ± 5.9 %, using a S:L ratio of 150 $mg.mL^{-1}$, pH 7 and a contact time of 30 min. Finally, for $[Si][N_{3888}]Cl$, the IgG is also adsorbed onto the material with a yield of 42.8 ± 0.7 % and a purity of 81.1 ± 8.9 %, using a S:L ratio of 50 $mg.mL^{-1}$, pH 7 and a contact time of 90 min. At pH 3, $[Si][C_3mim]Cl$ and IgG are positively charged, thus promoting a preferential capture of the protein impurities in the SIL and allowing IgG to be recovered in a simple and quick way, i.e. directly in the aqueous solution that contacted with the material. Also, $[Si][C_3mim]Cl$ presents an aromatic ring on its structure, and thus $\pi\ldots\pi$ interactions between the aromatic ring of the SIL and the aromatic residues of protein impurities may be playing a role in the process. On the other hand, by using $[Si][N_{3444}]Cl$ and $[Si][N_{3888}]Cl$ at pH 7, IgG is positively charged, while both SILs are negatively charged, being observed in this case a preferential adsorption of IgG onto the material. However, since a minor amount of HSA is also adsorbed in these conditions, along with electrostatic interactions (as discussed above), dispersive interactions may also be playing a role in the adsorption process. $[Si][N_{3444}]Cl$ and $[Si][N_{3888}]Cl$ are composed of long alkyl chains and are, consequently, the most hydrophobic SILs under study, whereas IgG is the most hydrophobic protein in the biological matrix (i.e. the protein composed of higher number of surface hydrophobic residues [47]).

The experimental data obtained in the 2^3 factorial plannings (response surface and contour plots) regarding the optimization of IgG recovery yield and purity are depicted in Fig. 3 and Fig. 4, respectively. The best conditions above mentioned for $[Si][C_3mim]Cl$ are close to the optimum zone (dark red), whereas for $[Si][N_{3444}]Cl$ and $[Si][N_{3888}]Cl$ they fit within the optimum zone obtained in the response surface and contour plots. Still, based on response surface plots, it is possible to predict the optimal conditions of S:L ratio, pH and contact time that allow to maximize IgG recovery yield and purity. The values of optimum conditions are summarized in the Supplementary Material (Table S22).

There is a close agreement between the optimum conditions for both the IgG recovery yield and IgG purity for $[Si][N_{3444}]Cl$ and $[Si][N_{3888}]Cl$, while a pH difference was observed for $[Si][C_3mim]Cl$. By the analysis of the pareto charts from $[Si][C_3mim]Cl$ [*cf.* Supplementary Material (Fig. S12 (A) and Fig. S13 (A))] it is shown that pH displays a significant influence upon the IgG recovery yield, and that no parameters appear to affect IgG purity. For $[Si][N_{3444}]Cl$ [*cf.* Supplementary Material (Fig. S12 (B) and Fig. S13 (B))], the pH significantly affects IgG recovery yield. Furthermore, also the pH quadratic function and the quadratic function of contact time are statistically relevant for the IgG purity. Finally, for $[Si][N_{3888}]Cl$ [*cf.* Supplementary Material (Fig. S12 (C) and Fig. S13 (C))], both pH and S:L ratio display a significant
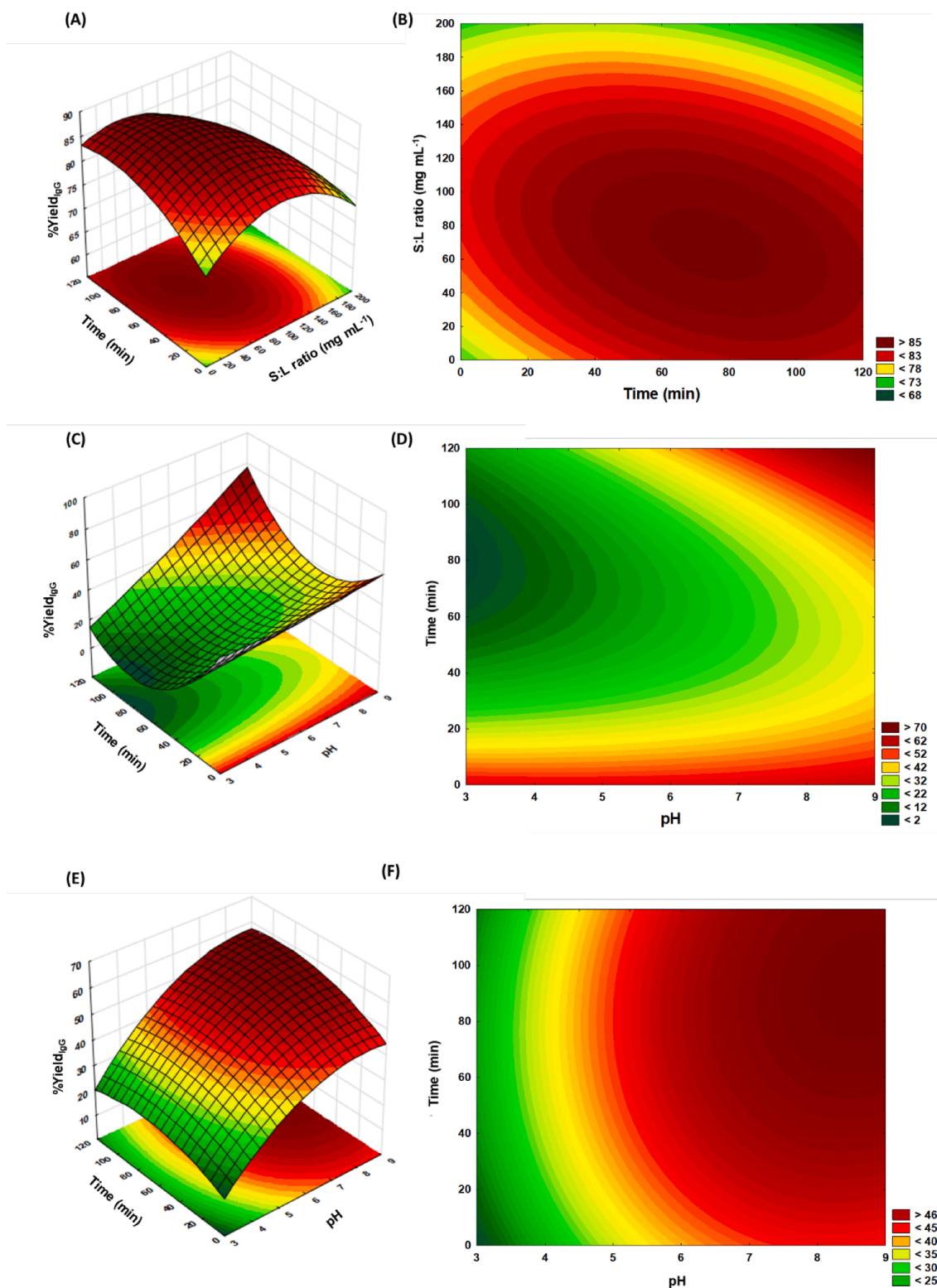
Fig. 3. Response surface plots (left) and contour plots (right) on the IgG recovery yield (%Yield$_{IgG}$) using: (A) and (B) [Si][C$_3$mim]Cl (focused on pH 5); (C) and (D) [Si][N$_{3444}$]Cl (focused on S:L ratio of 100 mg.mL^{-1}); and (E) and (F) [Si][N$_{3888}$]Cl (focused on S:L ratio of 100 mg.mL^{-1}).

influence in the IgG recovery yield, whereas only the pH affects significantly the IgG purity.

Overall, the pH is the most important and statistically relevant variable ruling the IgG recovery/purification process. Moreover, it was found that the central point was appropriate for the optimization of the IgG recovery yield using [Si][C$_3$mim]Cl, since the area of maximum

yield is included in the defined intervals; however, the factorial planning using the same materials for the optimization of IgG purity only allowed to define a region in which the IgG purification seems to be maximized (but with an undefined optimum point). Only slight discrepancies were identified between the predicted and experimental values for the recovery yield and purity of IgG [*cf.* Supplementary Material (Fig. S6 and
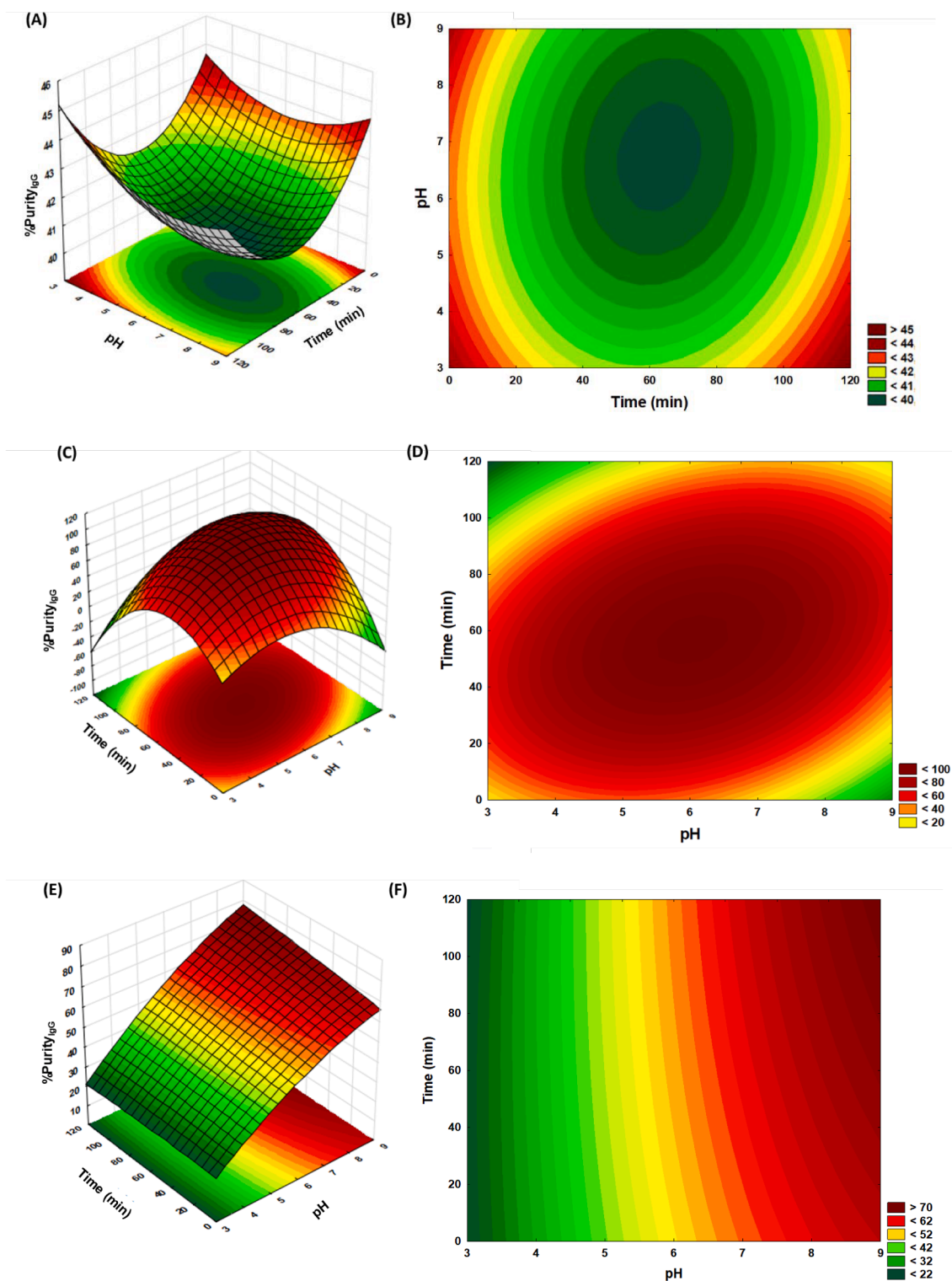
Fig. 4. Response surface plots (left) and contour plots (right) on the IgG purity level (%Purity$_{IgG}$) using: (A) and (B) [Si][C$_3$mim]Cl (focused on pH 5); (C) and (D) [Si][N$_{3444}$]Cl (focused on S:L ratio of 100 mg.mL^{-1}); and (E) and (F) [Si][N$_{3888}$]Cl (focused on S:L ratio of 100 mg.mL^{-1}).

Fig. S7)], assuring the accuracy and precision of the factorial design, and allowing to define as the optimum conditions for this material a S:L ratio of 50 mg.mL^{-1}, pH 3 and a contact time of 90 min. For the remaining SILs, [Si][N$_{3444}$]Cl and [Si][N$_{3888}$]Cl, some discrepancies for the recovery yield and purity of IgG were also identified between the predicted and experimental values [*cf.* Supplementary Material (Figs. S8-S11)], but it is still possible to clearly identify the most promising

conditions for the recovery and purification of IgG from human serum samples.

The obtained results through the studied factorial plannings allowed to identify the conditions required to achieve its maximum performance. In general, S:L ratios of 100 mg.mL^{-1}, more alkaline pH values (>8), and contact times above 60 min proved to be beneficial for the process.

3.5. Experimental optimization of the IgG purification process

Based on the results obtained from the factorial planning, the best conditions in terms of S:L ratio and contact time were fixed (100 mg. mL^{-1} and 60 min of contact time, in order to reduce the energetic input and the economic cost of the process), while the pH value, a parameter that was proven to be statistically significant, was further optimized to maximize the yield/purity of IgG from human serum samples. Since the factorial planning showed that alkaline pH values are more favourable for the processes under development, a pH study was carried out for all SILs, considering pH 10, 11 and 12. The stability of IgG at the selected alkaline pH range was evaluated by CD spectroscopy, whose spectra are shown in Fig. S14 in the Supplementary Material. The spectrum of IgG in PBS (pH 7.4) displays a minimum of ellipticity around 218 nm and a maximum at approximately 200 nm, which suggests the predominance of a β-sheet structure [51]. No noticeable changes in the spectra of IgG at pH values of 10, 11 and 12 were observed at wavelengths ranging from 210 to 260 nm, in comparison with that recorded at pH 7.4. A slight decrease of ellipticity was, however, observed for wavelengths within the range 200–205 nm, indicating a minor perturbation of the IgG secondary structure. Nevertheles, it does not impair its antigen binding activity, as addressed below by ELISA experiments.

The purification processes were investigated under the described conditions and data were analysed in terms of performance parameters (%Yield$_{IgG}$ and %Purity$_{IgG}$) for each material after contact with human serum samples, whose results are presented in Fig. 5. The detailed obtained data ([IgG], %Yield$_{IgG}$, %Purity$_{IgG}$ and %Purity$_{IgG}$) and the respective SE-HPLC chromatograms are given in the Supplementary Material (Table S23 and Figs. S15-S17, respectively).

It should be highlighted that, as previously described, using [Si] [C$_3$mim]Cl there is a preferential adsorption of the protein impurities onto the material whereas human IgG remains in solution, while using [Si][N$_{3444}$]Cl and [Si][N$_{3888}$]Cl the opposite behavior occurs. These different behaviors could be explained by the differences in the chemical structures of the SILs under study and the interactions they are capable to establish. Due to the different behaviors of the materials, the results shown in Fig. 5 reflect the performance parameters obtained in the aqueous medium for [Si][C$_3$mim]Cl and in the SIL material for [Si] [N$_{3444}$]Cl and [Si][N$_{3888}$]Cl.

In general, good recovery yields were achieved, ranging from a low value of 19.1 % up to 85.5 %, as well as promising purity levels, ranging from 40.7 % up to 100 %. It was found that pH 11 leads to the best compromise between recovery yield and purity level for all the three SILs studied. For instance, for [Si][C$_3$mim]Cl, an IgG recovery yield of 74.0 % and a purity level of 52.3 % were obtained in the aqueous medium, with a full removal of aggregates [%Aggregation$_{IgG}$ = 0.0 %, *cf.* the Supplementary Material (Table S23)]. Regarding [Si][N$_{3444}$]Cl, an extraction yield of 51.0 % was obtained with a purity level of 88.9 %, and with low aggregates content (%Aggregation$_{IgG}$ = 15.7 % vs 30.0 % in the initial human serum sample). Remarkably, the complete purification of IgG was achieved (100 %) in a single step using [Si][N$_{3888}$]Cl, with a recovery yied of 75.5 %, and also with low content in aggregates (%Aggregation$_{IgG}$ = 15.9 % vs 30.0 % in the initial human serum sample).

Based on the aforementioned information, the most hydrophobic SIL, [Si][N$_{3888}$]Cl, performs better than [Si][N$_{3444}$]Cl, since a good IgG recovery and complete purification (%Yield$_{IgG}$ = 75.5 %; %Purity$_{IgG}$ = 100 %) was achieved under the operating conditions studied – S:L ratio of 100 mg.mL^{-1}, pH 11, contact time of 60 min. Using [Si][C$_3$mim]Cl, a good recovery of IgG was obtained (74.0 %); however, with a purity of only 52.3 %. Since this material allowed the target protein, IgG, to remain in the liquid phase, and thus a different operation mode, this material was selected to proceed with studies after an optimization of the S:L ratio aiming to maximize the performance parameters.

The process based on [Si][C$_3$mim]Cl, that would allow a simple and direct recovery of IgG in the aqueous media without any elution step, was optimized concerning the S:L ratio (100, 150 and 200 mg.mL^{-1}), at different pH values (pH 10, 11 and 12) and at a fixed contact time of 60 min. The results obtained (%Yield$_{IgG}$ and %Purity$_{IgG}$) are shown in Fig. 6, whereas the detailed obtained data ([IgG], %Yield$_{IgG}$, %Purity$_{IgG}$ and %Purity$_{IgG}$) can be found in the Supplementary Material (Table S24).

Recovery yields ranging between 54.5 % and 88.2 % with purity levels comprised between 31.3 % and up to 84.2 % were achieved in a single step. Moreover, independently of the S:L ratio used, higher recovery yields were obtained for the lowest pH value (%Yield$_{IgG}$ ranging between 79.3 % and 88.2 %), while lower recovery yields for the highest pH value (%Yield$_{IgG}$ ranging between 54.5 % and 59.2 %). Nevertheless,
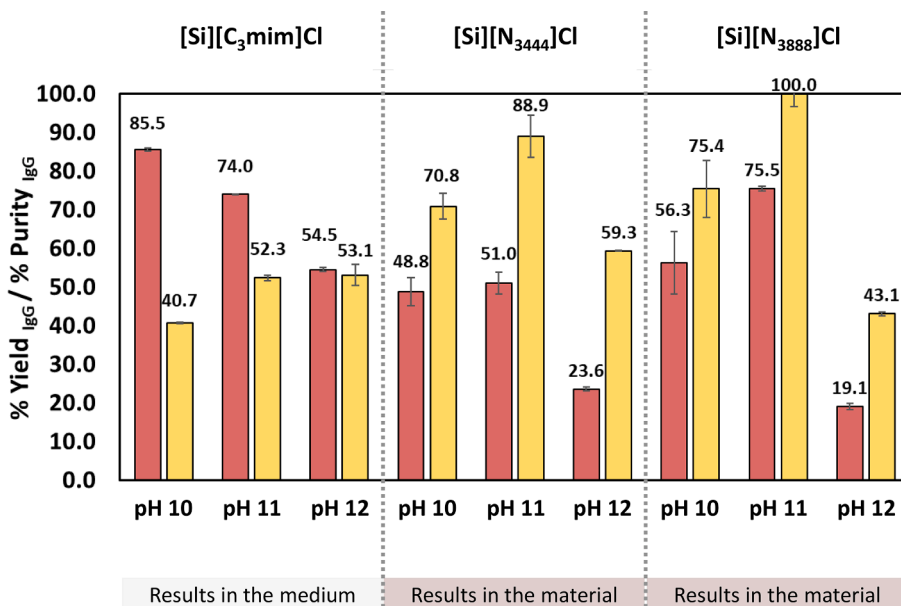

Fig. 5. Recovery yields (%Yield$_{IgG}$ – ■) and purity levels (%Purity$_{IgG}$ – ■) of human IgG from serum samples after contact with SILs materials ([Si][C$_3$mim]Cl, [Si] [N$_{3444}$]Cl and [Si][N$_{3888}$]Cl), using the following operation conditions: S:L ratio of 100 mg.mL^{-1}, three different pH values (pH 10, 11 and 12) and 60 min of contact time.
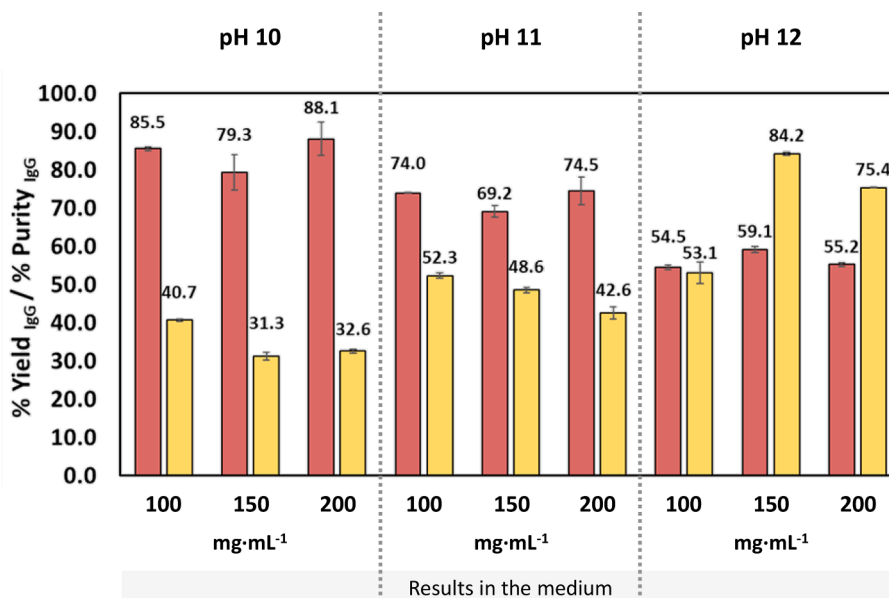
Fig. 6. Recovery yields (%Yield$_{IgG}$ – ■) and purity levels (%Purity$_{IgG}$ – ■) of human IgG from serum samples after contact with [Si][C$_3$mim]Cl, using the following operation conditions: S:L ratio of 100, 150 and 200 mg.mL^{-1}, three different pH values (pH 10, 11 and 12) and 60 min of contact time.

it is interesting to notice that an opposite trend was observed regarding the purity of IgG, which increases with the pH value, allowing purity levels up to 84.2 % to be achieved at pH 12. It is important to highlight that the increase of the S:L ratio from 100 up to 200 mg.mL^{-1} for pH 10 and 11 leads to a decrease in the purity levels of IgG (from 40.7 % to 32.6 %, and from 52.3 % to 42.6 %, respectively), thus revealing not to favour the IgG purification process. However, at pH 12, the increase in the S:L ratio showed to have an important role on the purification process, since an increase on the IgG purity level was observed for higher S:

L ratios. The best results in terms of compromise between recovery yield and purity were obtained at pH 12 and using a S:L ratio of 150 mg.mL^{-1}, allowing to recover 59.2 % of IgG from human serum with a purity level of 84.2 % in a single-step. Under these conditions, the influence of the purification process on the secondary structure of IgG was evaluated by CD spectroscopy, being the recorded spectra displayed in Fig. S18 (Supplementary Material). As expected, the CD spectrum of HSA shows two minima of ellipticity at 208 and 222 nm, being characteristic of their α-helical structure [52]. Also, the CD spectrum of human serum at pH 12
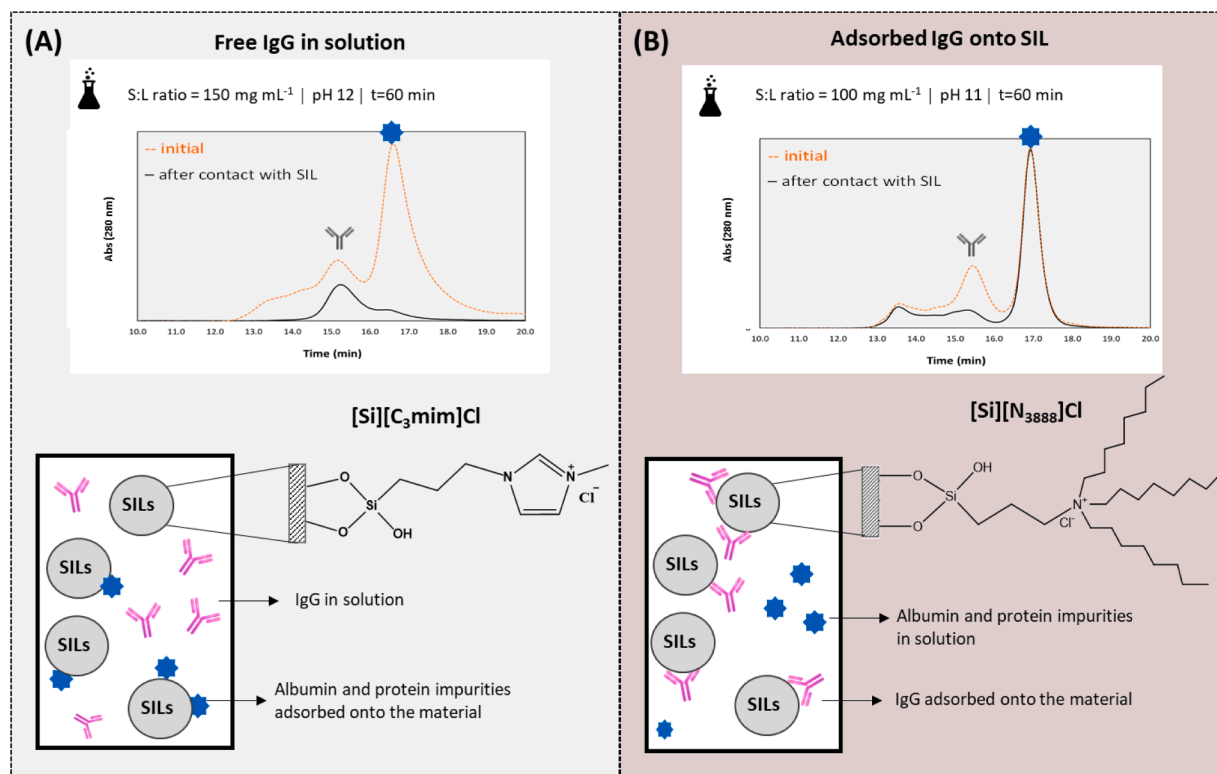

Fig. 7. Schematic overview on the proposed IgG recovery and purification processes mediated by SILs: (A) Albumin and protein impurities adsorbed on [Si][C$_3$mim] Cl while IgG remains in solution; and (B) IgG is adsorbed onto [Si][N$_{3888}$]Cl while albumin and other protein impurities remain in solution.

largely resembles that of HSA, indicating the predominance of this protein over IgG. However, we noticed that the CD spectrum of IgG purified using [Si][C$_3$mim]Cl is similar to that of the standard IgG, with a minor deviation in the wavelength at which the minimum of ellipticity is achieved. Overall, these results not only demonstrate that IgG retains, in general, its native secondary structure during the purification process, as it is effectively obtained in a more purified form than that initially found in the human serum.

Based on the exposed, it was possible to optimize the SIL-mediated process with [Si][C$_3$mim]Cl in order to show a good performance towards IgG recovery and purification with its native secondary structure, having the advantage that IgG can be simply and directly recovered in the aqueous medium after contact with the SIL material.

Based on the aforementioned results, two different IgG recovery/purification approaches can be followed, depending on the chemical structure of the IL supported in the silica material. SILs may be designed to allow both the selective adsorption of IgG or the selective adsorption of other proteins present in the media. The two different strategies are schematically presented in Fig. 7.

It is shown that IgG can be purified and recovered in a very simple and direct way in the aqueous medium after contact with [Si][C$_3$mim]Cl, under specific operation conditions (S:L ratio of 150 mg.mL^{-1}, pH 12, and contact time of 60 min). In this case, it is possible to adsorb the protein impurities onto the SIL material, in particular albumin, as well as high molecular weight protein aggregates, while IgG remain in the aqueous media. Through the SE-HPLC chromatogram presented in Fig. 7 (A), it is noticeable the predominance of the IgG peak in the sample after contact with the SIL material, confirming its presence with a high purity level in the aqueous solution (recovery yield of 59.2 % and purity level of 84.2 %), and free of protein aggregates. Imidazolium-based ILs already proved to improve the results achieved for the downstream processing of antibodies with other techniques, namely as adjuvants in aqueous biphasic systems [53], where an IgG extraction yield of 46 % and a purity level of 26 % were obtained. Still, the results obtained in this work using the imidazolium-based SIL seems to be promising with a better performance.

On the other hand, IgG could be adsorbed onto [Si][N$_{3888}$]Cl, leading to the protein impurities to be retained in the aqueous media, under specific operation conditions (S:L ratio of 100 mg.mL^{-1}, pH 11, and contact time of 60 min). Under these operation conditions, 75.5 % of IgG could be recovered with a purity of 100 %, in a single-step, and with a reduction of the protein aggregates to 15.9 % (*cf.* the SE-HPLC chromatogram in Fig. 7 (B)). Taking into account the initial concentration of IgG in human serum, the mass of [Si][N$_{3888}$]Cl and the IgG yield after adsorption, the amount of IgG adsorbed *per* weight of material is 3.55 mg IgG.g^{-1} [Si][N$_{3888}$]Cl. The results herein reported are better than those obtained with the same type of ILs (quaternary ammonium-based ILs) in other techniques, such as aqueous micellar two-phase systems (AMTPS) [54] applied to the purification of IgG from human plasma. Vicente et al. [54] reported a slightly higher recovery yield of 82 % (vs 76 % obtained in this work using [Si][N$_{3888}$]Cl), however, with a lower purification factor. Affinity chromatography, namely Protein A affinity, is one of the commonly used techniques for antibody purification due to its high selectivity to IgG (high purity, > 90 %) from complex biological sources [55,56]. However, there is an urgent demand towards the development of novel chromatographic resins with improved stability, which will be essential to decrease the purification costs.

Overall, SILs appear as promising candidates for the development of cost-effective alternatives for the downstream processing of therapeutic antibodies that deserve to be studied in the future as chromatographic matrices, with envisaged potential to work on the flowthrough or bind-and-elute modes according to the chosen IL chemical structure. In comparison with common affinity ligands, it is herein demonstrated that SILs maintain their ability to establish a multitude of interactions with IgG and remarkable purification performance, further displaying improved stability in wide operating conditions, such as in an extended

range of pH values. Therefore, the ability to easily fine-tuning the chemical structure of SILs toward improved purification processes coupled with their high stability strongly support their application as efficient alternative materials for the capture and purification of IgG.

3.6. Reproducibility and robustness of the developed processes

To evaluate the reproducibility and robustness of the proposed SILs for processing other complex biological matrices, additional studies were carried out using CHO cell culture supernatants and rabbit serum samples (20-fold diluted). The studies were carried out under the best operation conditions identified for the two most promising SILs: [Si][C$_3$mim]Cl (S:L ratio of 150 mg.mL^{-1}, pH 12, and contact time of 60 min) and [Si][N$_{3888}$]Cl (S:L ratio of 100 mg.mL^{-1}, pH 11, and contact time of 60 min). The results obtained (%Yield$_{IgG}$ and %Purity$_{IgG}$) are shown in Fig. 8, whereas the detailed data obtained ([IgG], %Yield$_{IgG}$, % Purity$_{IgG}$ and %Purity$_{IgG}$) are provided in the Supplementary Material (Table S25). The chromatograms for the human serum, CHO cell culture supernatants and rabbit serum are given in the Supplementary Material (Figs. S19 and S20).

Although dealing with different biological samples, that inherently display different compositions, the obtained results show that, in general, similar trends are obtained. For [Si][C$_3$mim]Cl, independently of the biological matrix, the IgG remains in solution after contact with the SIL adsorbent. When bioprocessing the two new biological matrices, higher IgG recovery yields are obtained (>75 %) in comparison with human serum (59.2 %); however, with lower purity values (<52 %). In particular, for the rabbit serum samples, 75.7 % of IgG could be recovered with a purity level of 51.4 %, and when bioprocessing CHO cell culture supernatants, a higher recovery yield is achieved (85.8 %) even though with a lower purity (36.8 %). The performance of the purification processes developed for distinct biological samples using [Si][C$_3$mim]Cl were also analysed by denaturing and reducing protein electrophoresis, as shown in Fig. S21 (Supplementary Material). Although with varying contents, the major impurity in all biological samples is albumin, while IgG is composed of two heavy chains and two light chains, visible in reducing SDS-PAGE, respectively, with molecular weights of 50 kDa and 25 kDa. As observed in the SDS-PAGE gel, there is a depletion of albumin after the contact of the biological sample with the SIL, being this effect more pronounced for human serum. As a result, the purity of IgG recovered in the aqueous medium recovered after the incubation of the SIL with human serum is higher than that recovered with rabbit serum and the CHO cell supernatant, being also in good agreement with the results displayed in Fig. 8.

Competitive ELISA was also applied to qualitatively evaluate if the purified mAbs from CHO cell culture supernatants retain their biological activity, a parameter deemed crucial to ensure their therapeutic efficiency. As demonstrated in Table S26 (Supplementary Material), in comparison with the blank (negative control), the mouse anti-human CXCL8/IL8 antibody (positive control) and the CHO cell supernatants and purified mAbs samples present lower absorbance values. Being a competitive ELISA experiment, the presence of biologically active anti-IL-8 mAbs in the analysed samples will impair binding of human IL-8 conjugate to IL-8, and hence less substrate is transformed in the coloured product, accounting for the reduction in the absorbance at 450 nm. In summary, competitive ELISA experiments confirm that no noticeable conformational changes in IgG occur during the purification process.

Regarding the bioprocess mediated by [Si][N$_{3888}$]Cl, and for the new matrices, IgG was evenly distributed between the SIL and the aqueous media, since a recovery yield of around 50 % was achieved in both cases. Particularly, a recovery yield of 49.8 % with a purity of 96.4 % was achieved in the material for rabbit serum, and a recovery yield of 48.1 % with a purity of 64.9 % was achieved in the material for the CHO cell culture supernatant.

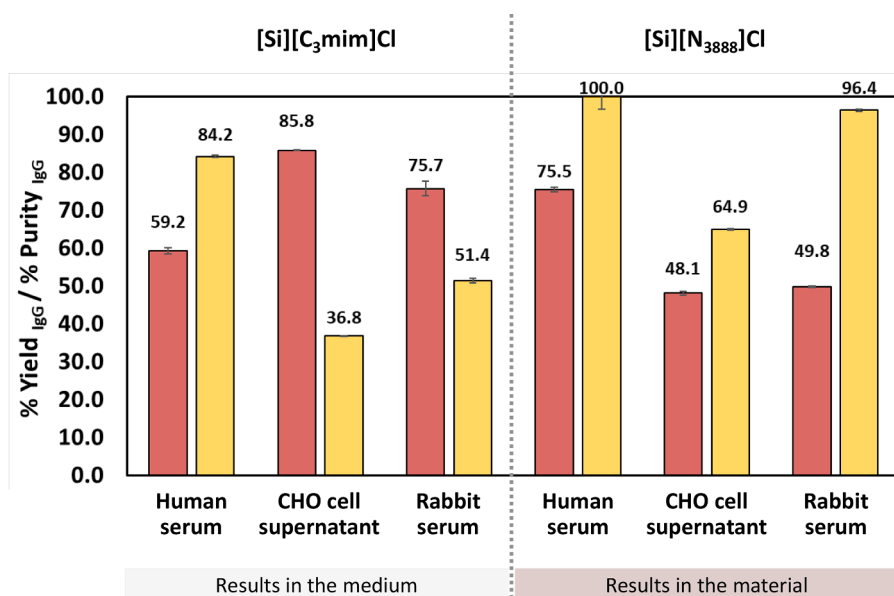Although in general lower performance parameters were obtained

Fig. 8. Recovery yields (%Yield$_{IgG}$ – ■) and purity levels (%Purity$_{IgG}$ – ■) of IgG from different biological matrices (human serum, CHO cell culture supernatants and rabbit serum) after contact with [Si][C$_3$mim]Cl (operation conditions: S:L ratio of 150 mg.mL^{-1}, pH 12 and 60 min of contact time) and [Si][N$_{3888}$]Cl (operation conditions: S:L ratio of 100 mg.mL^{-1}, pH 11 and 60 min of contact time).

for the new matrices than those achieved for human serum samples, it should be remarked that a similar yield/purity level was observed for rabbit serum – a matrix with higher similarity to human serum than cell culture supernatants. In the CHO cell culture supernatant, the major protein impurity is BSA whereas other protein impurities are also present resulting from the medium used in the cell proliferation, growth, and also from their metabolism (e.g. insulin, transferrin and other CHO host cell proteins) [48]. Therefore, it can be concluded that the same adsorption mechanisms were present in each SIL, independently of the matrix under study. Although a lower performance was found when bioprocessing other matrices than human serum, good results for the recovery yield/purity have been however found. Improvements in the performance of SIL-mediated downstream processes for other complex biological matrices such as rabbit serum or CHO cell culture supernatants, would require the optimization of the operational parameters for each matrix. Even though not addressed in this work, the regeneration and reuse of SILs was previously demonstrated [40,57] following appropriated clean-in-place (CIP) procedures, reinforcing the possibility that the materials investigated in this work could be recycled and reused as well. Moreover, it should be highlighted that the material with the best performance for IgG purification, [Si][N$_{3888}$]Cl, presents a negligible toxicity towards the liver cell line HepG2 [39].

4. Conclusions

Aiming to develop new recovery/purification platforms for therapeutic IgG antibodies from complex biological media, the potential of SILs as alternative purification materials was here evaluated. Three SILs ([Si][C$_3$mim]Cl, [Si][N$_{3444}$]Cl and [Si][N$_{3888}$]Cl) were synthesized, characterized and studied for the first time towards the recovery and purification of IgG antibodies from biological matrices. Firstly, an initial screening of pH values (from 3.0 to 9.0) was performed to evaluate the effect of the pH in the (selective) adsorption of proteins from human serum. A pH equal to 5 or higher is required for proteins adsorption. Then, a factorial planning was implemented to get insights regarding the optimum conditions to purify IgG, namely in terms of S:L ratio, pH and contact time. Based on the results obtained, a S:L ratio of 100 mg.mL^{-1}, a pH higher than 9, and a contact time of 60 min were identified as the optimum conditions for a better performance of the SIL-mediated processes. The performance parameters were then optimized through the

optimization of the pH value and S:L ratio.

Two different IgG recovery/purification mechanisms were identified, being highly dependent on the IL chemical structure: (i) by using [Si][C$_3$mim]Cl, IgG could be simply and directly recovered in the aqueous solution after contact with the material under a specific set of operating conditions, namely an S:L ratio of 150 mg.mL^{-1}, pH 12, and a contact time of 60 min, yielding 59 % of IgG with a purity level of 84 %; and (ii) by using [Si][N$_{3888}$]Cl, IgG is mainly adsorbed onto the material, using as operating conditions an S:L ratio of 100 mg·mL^{-1}, pH 11 and contact time of 60 min, yielding 76 % of IgG with a purity level of 100 %. The identified conditions were applied for the downstream processing of IgG antibodies from other complex biological matrices, namely CHO cell culture supernatants and rabbit serum, revealing the same recovery/purification mechanisms. It is further demonstrated that the secondary structure of purified IgG in the aqueous medium after contact with [Si][C$_3$mim]Cl is generally preserved during purification, while the biological activity of anti-IL-8 mAbs recovered from the CHO cell supernatant retain their biological activity. These features are crucial parameters considering that they will influence the therapeutic efficiency of purified antibodies using these materials.

Overall, it is shown that by only changing the IL chemical structure, SILs are customizable materials, being able to establish a multitude of interactions with the target biopharmaceuticals and with future potential to work as chromatographic columns in the flowthrough or bind-and-elute modes to capture and purify IgG. SILs are of low-cost and display improved stabilities in wide operating conditions, thus having high potential to substitute commercial chromatographic columns currently used in preparative liquid chromatography based on biological ligands to purify IgG. Based on the results here reported it is expected to have SILs being adopted by the pharmaceutical industry as novel chromatographic matrices.

CRediT authorship contribution statement

Emanuel V. Capela: Methodology, Data curation, Validation, Writing – original draft. **Jéssica Bairos:** Methodology, Data curation. **Augusto Q. Pedro:** Methodology, Data curation, Investigation, Validation, Writing – review & editing. **Márcia C. Neves:** Methodology, Data curation, Investigation, Validation. **M. Raquel Aires-Barros:** Supervision, Funding acquisition. **Ana M. Azevedo:** Supervision, Funding

acquisition. **João A.P. Coutinho:** Supervision, Project administration, Investigation, Funding acquisition, Writing – review & editing. **Ana P. M. Tavares:** Methodology, Data curation, Investigation, Validation, Writing – review & editing. **Mara G. Freire:** Conceptualization, Supervision, Project administration, Methodology, Resources, Funding acquisition, Investigation, Writing – review & editing.

Declaration of Competing Interest

The authors declare that they have no known competing financial interests or personal relationships that could have appeared to influence the work reported in this paper.

Data availability

Data will be made available on request.

Appendix A. Supplementary material

Supplementary data to this article can be found online at https://doi. org/10.1016/j.seppur.2022.122464.

References

[1] A.M. Azevedo, P.A.J. Rosa, I.F. Ferreira, J. de Vries, T.J. Visser, M.R. Aires-Barros, Downstream processing of human antibodies integrating an extraction capture step and cation exchange chromatography, J. Chromatogr. B. 877 (1-2) (2009) 50–58.

[2] S. Fekete, A. Goyon, J. Veuthey, D. Guillarme, Size exclusion chromatography of protein biopharmaceuticals: past, present and future, Am. Pharm. Rev. 21 (2018) 1–4.

[3] M. Vargas, Á. Segura, M. Herrera, M. Villalta, Y. Angulo, J.M. Gutiérrez, G. León, T. Burnouf, Purification of IgG and albumin from human plasma by aqueous two phase system fractionation, Biotechnol. Prog. 28 (2012) 1005–1011, https://doi. org/10.1002/BTPR.1565.

[4] J.M. Dwyer, Intravenous therapy with gamma globulin, Adv. Intern. Med. 32 (1987) 111–135. http://europepmc.org/abstract/MED/3548246.

[5] J. Daller, Biosimilars: A consideration of the regulations in the United States and European union, Regul. Toxicol. Pharmacol. 76 (2016) 199–208, https://doi.org/10.1016/J.YRTPH.2015.12.013.

[6] G. Singh, K. Komal, M. Singh, O. Singh, T.S. Kang, Hydrophobically driven morphologically diverse self-assembled architectures of deoxycholate and imidazolium-based biamphiphilic ionic liquids in aqueous medium, J. Phys. Chem. B. 122 (2018) 12227–12239, https://doi.org/10.1021/acs.jpcb.8b10161.

[7] A.C.A. Roque, C.R. Lowe, M.Â. Taipa, Antibodies and genetically engineered related molecules: production and purification, Biotechnol. Prog. 20 (2004) 639–654, https://doi.org/10.1021/BP030070K.

[8] A.L. Grilo, M. Mateus, M.R. Aires-Barros, A.M. Azevedo, Monoclonal antibodies production platforms: an opportunity study of a non-protein-a chromatographic platform based on process economics, Biotechnol. J. 12 (2017) 1700260, https://doi.org/10.1002/BIOT.201700260.

[9] E. V. Capela, M.R. Aires-Barros, M.G. Freire, A.M. Azevedo, Monoclonal antibodies - addressing the challenges on the manufacturing processing of an advanced class of therapeutic agents, in: Benthan Science, 2017: pp. 142–203. https://doi.org/10.2174/9781681084879117040007.

[10] S.-Y. Jing, J.-X. Gou, D. Gao, H.-B. Wang, S.-J. Yao, D.-Q. Lin, Separation of monoclonal antibody charge variants using cation exchange chromatography: resins and separation conditions optimization, Sep. Purif. Technol. 235 (2020), 116136, https://doi.org/10.1016/J.SEPPUR.2019.116136.

[11] G. Joucla, C. Le Sénéchal, M. Bégorre, B. Garbay, X. Santarelli, C. Cabanne, Cation exchange versus multimodal cation exchange resins for antibody capture from CHO supernatants: identification of contaminating Host Cell Proteins by mass spectrometry, J. Chromatogr. B. 942–943 (2013) 126–133, https://doi.org/10.1016/J.JCHROMB.2013.10.033.

[12] Y. Hou, M. Brower, D. Pollard, D. Kanani, R. Jacquemart, B. Kachuik, J. Stout, Advective hydrogel membrane chromatography for monoclonal antibody purification in bioprocessing, Biotechnol. Prog. 31 (2015) 974–982, https://doi.org/10.1002/BTPR.2113.

[13] R. Ghosh, L. Wang, Purification of humanized monoclonal antibody by hydrophobic interaction membrane chromatography, J. Chromatogr. A. 1107 (2006) 104–109, https://doi.org/10.1016/j.chroma.2005.12.035.

[14] L. Guerrier, I. Flayeux, E. Boschetti, A dual-mode approach to the selective separation of antibodies and their fragments, J. Chromatogr. B. Biomed. Sci. Appl. 755 (2001) 37–46, https://doi.org/10.1016/S0378-4347(00)00598-3.

[15] S. Vançan, E.A. Miranda, S.M.A. Bueno, IMAC of human IgG: Studies with IDA-immobilized copper, nickel, zinc, and cobalt ions and different buffer systems, Process Biochem. 37 (2002) 573–579, https://doi.org/10.1016/S0032-9592(01)00242-4.

[16] Y. González, N. Ibarra, H. Gómez, M. González, L. Dorta, S. Padilla, R. Valdés, Expanded bed adsorption processing of mammalian cell culture fluid: comparison with packed bed affinity chromatography, J. Chromatogr. B. 784 (2003) 183–187, https://doi.org/10.1016/S1570-0232(02)00712-2.

[17] R. Giovannini, R. Freitag, Isolation of a recombinant antibody from cell culture supernatant: continuous annular versus batch and expanded-bed chromatography, Biotechnol. Bioeng. 73 (2001) 522–529, https://doi.org/10.1002/BIT.1087.

[18] Z.-Y. Gao, Q.-L. Zhang, C.e. Shi, J.-X. Gou, D. Gao, H.-B. Wang, S.-J. Yao, D.-Q. Lin, Antibody capture with twin-column continuous chromatography: Effects of residence time, protein concentration and resin, Sep. Purif. Technol. 253 (2020), 117554, https://doi.org/10.1016/J.SEPPUR.2020.117554.

[19] C.P. Lin, K. Saito, R.I. Boysen, E.M. Campi, M.T.W. Hearn, Static and dynamic binding behavior of an IgG2 monoclonal antibody with several new mixed mode affinity adsorbents, Sep. Purif. Technol. 163 (2016) 199–205, https://doi.org/10.1016/J.SEPPUR.2016.02.048.

[20] S. Ghose, B. Hubbard, S.M. Cramer, Evaluation and comparison of alternatives to Protein A chromatography Mimetic and hydrophobic charge induction chromatographic stationary phases, J. Chromatogr. A. 1122 (2006) 144–152, https://doi.org/10.1016/J.CHROMA.2006.04.083.

[21] G. El Khoury, C.R. Lowe, A biomimetic protein G affinity adsorbent: an Ugi ligand for immunoglobulins and Fab fragments based on the third IgG-binding domain of Protein G, J. Mol. Recognit. 26 (2013) 190–200, https://doi.org/10.1002/JMR.2265.

[22] T. Arakawa, Y. Kita, H. Sato, D. Ejima, MEP chromatography of antibody and Fc-fusion protein using aqueous arginine solution, Protein Expr. Purif. 63 (2009) 158–163, https://doi.org/10.1016/J.PEP.2008.09.011.

[23] Y. Liu, Y. Lu, Z. Liu, Restricted access boronate affinity porous monolith as a protein A mimetic for the specific capture of immunoglobulin G, Chem. Sci. 3 (2012) 1467–1471, https://doi.org/10.1039/C2SC20125A.

[24] C.S.M. Fernandes, R. dos Santos, S. Ottengy, A.C. Viecinski, G. Bhar, B. Mouratou, F. Pecorari, A.C. Roque, Affitins for protein purification by affinity magnetic fishing, J. Chromatogr. A. 1457 (2016) 50–58, https://doi.org/10.1016/j.chroma.2016.06.020.

[25] B.M. Alves, L. Borlido, S.A.S.L. Rosa, M.F.F. Silva, M.R. Aires-Barros, A.C.A. Roque, A.M. Azevedo, Purification of human antibodies from animal cell cultures using gum arabic coated magnetic particles, J. Chem. Technol. Biotechnol. 90 (2015) 838–846, https://doi.org/10.1002/jctb.4378.

[26] M.J.B. Matos, F. Trovão, J. Gonçalves, U. Rothbauer, M.G. Freire, A.M.J. B. Barbosa, A.S. Pina, A.C.A. Roque, A purification platform for antibodies and derived fragments using a de novo designed affinity adsorbent, Sep. Purif. Technol. 265 (2021) 118476, https://doi.org/10.1016/J.SEPPUR.2021.118476.

[27] N. Fontanals, S. Ronka, F. Borrull, A.W. Trochimczuk, R.M. Marcé, Supported imidazolium ionic liquid phases: a new material for solid-phase extraction, Talanta. 80 (2009) 250–256, https://doi.org/10.1016/J.TALANTA.2009.06.068.

[28] T.D. Ho, A.J. Canestraro, J.L. Anderson, Ionic liquids in solid-phase microextraction: a review, Anal. Chim. Acta. 695 (2011) 18–43, https://doi.org/10.1016/J.ACA.2011.03.034.

[29] L. Vidal, M.L. Riekkola, A. Canals, Ionic liquid-modified materials for solid-phase extraction and separation: a review, Anal. Chim. Acta. 715 (2012) 19–41, https://doi.org/10.1016/J.ACA.2011.11.050.

[30] N. Fontanals, F. Borrull, R.M. Marcé, Ionic liquids in solid-phase extraction, TrAC - Trends Anal. Chem. 41 (2012) 15–26, https://doi.org/10.1016/j.trac.2012.08.010.

[31] D.H. Cheng, X.W. Chen, Y. Shu, J.H. Wang, Selective extraction/isolation of hemoglobin with ionic liquid 1-butyl-3-trimethylsilylimidazolium hexafluorophosphate (BtmsimPF6), Talanta. 75 (2008) 1270–1278, https://doi.org/10.1016/J.TALANTA.2008.01.044.

[32] P. Du, S. Liu, P. Wu, C. Cai, Preparation and characterization of room temperature ionic liquid/single-walled carbon nanotube nanocomposites and their application to the direct electrochemistry of heme-containing proteins/enzymes, Electrochim. Acta. 52 (2007) 6534–6547, https://doi.org/10.1016/j.electacta.2007.04.092.

[33] N.A. Ramli, N.A. Hashim, M.K. Aroua, Supported ionic liquid membranes (SILMs) as a contactor for selective absorption of CO2/O2 by aqueous monoethanolamine (MEA), Sep. Purif. Technol. 230 (2020), 115849, https://doi.org/10.1016/J.SEPPUR.2019.115849.

[34] H. Qiu, S. Jiang, X. Liu, L. Zhao, Novel imidazolium stationary phase for high-performance liquid chromatography, J. Chromatogr. A. 1116 (2006) 46–50, https://doi.org/10.1016/J.CHROMA.2006.03.016.

[35] H. Qiu, S. Jiang, X. Liu, N-Methylimidazolium anion-exchange stationary phase for high-performance liquid chromatography, J. Chromatogr. A. 1103 (2006) 265–270, https://doi.org/10.1016/J.CHROMA.2005.11.035.

[36] Q. Wang, G.A. Baker, S.N. Baker, L.A. Colón, Surface confined ionic liquid as a stationary phase for HPLC, Analyst. 131 (2006) 1000–1005, https://doi.org/10.1039/B607337A.

[37] S. Van Roosendael, M. Regadío, J. Roosen, K. Binnemans, Selective recovery of indium from iron-rich solutions using an Aliquat 336 iodide supported ionic liquid phase (SILP), Sep. Purif. Technol. 212 (2019) 843–853, https://doi.org/10.1016/J.SEPPUR.2018.11.092.

[38] M. Van de Voorde, K. Van Hecke, K. Binnemans, T. Cardinaels, Supported ionic liquid phases for the separation of samarium and europium in nitrate media: Towards purification of medical samarium-153, Sep. Purif. Technol. 232 (2020), 115939, https://doi.org/10.1016/J.SEPPUR.2019.115939.

[39] S.C. Bernardo, B.R. Araújo, A.C.A. Sousa, R.A. Barros, A.C. Cristovão, M.C. Neves, M.G. Freire, Supported ionic liquids for the efficient removal of acetylsalicylic acid from aqueous solutions, Eur. J. Inorg. Chem. 2020 (2020) 2380–2389, https://doi.org/10.1002/ejic.202000101.

[40] H.F.D. Almeida, M.C. Neves, T. Trindade, I.M. Marrucho, M.G. Freire, Supported ionic liquids as efficient materials to remove non-steroidal anti-inflammatory drugs from aqueous media, Chem. Eng. J. 381 (2020), 122616, https://doi.org/10.1016/J.CEJ.2019.122616.

[41] Y. Shu, X.W. Chen, J.H. Wang, Ionic liquid-polyvinyl chloride ionomer for highly selective isolation of basic proteins, Talanta. 81 (2010) 637–642, https://doi.org/10.1016/j.talanta.2009.12.059.

[42] G. Zhao, S. Chen, X.W. Chen, R.H. He, Selective isolation of hemoglobin by use of imidazolium-modified polystyrene as extractant, Anal. Bioanal. Chem. 405 (2013) 5353–5358, https://doi.org/10.1007/s00216-013-6889-y.

[43] H. Song, C. Yang, A. Yohannes, S. Yao, Acidic ionic liquid modified silica gel for adsorption and separation of bovine serum albumin (BSA), RSC Adv. 6 (2016) 107452–107462, https://doi.org/10.1039/c6ra23372d.

[44] R. dos Santos, S.A.S.L. Rosa, M.R. Aires-Barros, A. Tover, A.M. Azevedo, Phenylboronic acid as a multi-modal ligand for the capture of monoclonal

[45] J.C.F. Nunes, M.R. Almeida, R.M.F. Bento, M.M. Pereira, V.C. Santos-Ebinuma, M. C. Neves, M.G. Freire, A.P.M. Tavares, Enhanced Enzyme Reuse through the Bioconjugation of L-Asparaginase and Silica-Based Supported Ionic Liquid-like Phase Materials, Mol. 2022, Vol. 27, Page 929. 27 (2022) 929. https://doi.org/10.3390/MOLECULES27030929.

[46] P. Hong, S. Koza, E.S.P. Bouvier, A review size-exclusion chromatography for the analysis of protein biotherapeutics and their aggregates, J. Liq. Chromatogr. Relat. Technol. 35 (2012) 2923–2950, https://doi.org/10.1080/10826076.2012.743724.

[47] P.A.J. Rosa, A.M. Azevedo, M.R. Aires-Barros, Application of central composite design to the optimisation of aqueous two-phase extraction of human antibodies, J. Chromatogr. A. 1141 (2007) 50–60, https://doi.org/10.1016/j.chroma.2006.11.075.

[48] E.V. Capela, A.E. Santiago, A.F.C.S. Rufino, A.P.M. Tavares, M.M. Pereira, A. Mohamadou, M.R.R. Aires-Barros, J.A.P. Coutinho, A.M. Azevedo, M.G. Freire, Sustainable strategies based on glycine-betaine analogue ionic liquids for the recovery of monoclonal antibodies from cell culture supernatants, Green Chem. 21 (2019) 5671–5682, https://doi.org/10.1039/c9gc02733e.

[49] C.C. Ramalho, C.M.S.S. Neves, M.V. Quental, J.A.P. Coutinho, M.G. Freire, Separation of immunoglobulin G using aqueous biphasic systems composed of cholinium-based ionic liquids and poly(propylene glycol), J. Chem. Technol. Biotechnol. 93 (2018) 1931–1939, https://doi.org/10.1002/jctb.5594.

[50] Y. Shu, M. Liu, S. Chen, X. Chen, J. Wang, New insight into molecular interactions of imidazolium ionic liquids with bovine serum albumin, J. Phys. Chem. B. 115 (2011) 12306–12314, https://doi.org/10.1021/jp2071925.

[51] D. Dhiman, M. Bisht, A.P.M. Tavares, M.G. Freire, P. Venkatesu, Cholinium-based ionic liquids as efficient media for improving the structural and thermal stability of immunoglobulin G antibodies, accessed May 28, 2022, ACS Sustain. Chem. Eng. 10 (2022), https://pubs.acs.org/doi/abs/10.1021/acssuschemeng.1c07979.

[52] A. Varlan, M. Hillebrand, Bovine and human serum albumin interactions with 3-carboxyphenoxathiin studied by fluorescence and circular dichroism spectroscopy, Molecules. 15 (2010) 3905–3919, https://doi.org/10.3390/MOLECULES15063905.

[53] A.M. Ferreira, V.F.M.M. Faustino, D. Mondal, J.A.P.P. Coutinho, M.G. Freire, Improving the extraction and purification of immunoglobulin G by the use of ionic liquids as adjuvants in aqueous biphasic systems, J. Biotechnol. 236 (2016) 166–175, https://doi.org/10.1016/j.jbiotec.2016.08.015.

[54] F.A. Vicente, J. Bairos, M. Roque, J.A.P. Coutinho, S.P.M. Ventura, M.G. Freire, Use of ionic liquids as cosurfactants in mixed aqueous micellar two-phase systems to improve the simultaneous separation of immunoglobulin g and human serum albumin from expired human plasma, ACS Sustain. Chem. Eng. 7 (2019) 15102–15113, https://doi.org/10.1021/acssuschemeng.9b03841.

[55] S. Hober, K. Nord, M. Linhult, Protein A chromatography for antibody purification, 848 (2007) 40–47.

[56] A.A. Shukla, B. Hubbard, T. Tressel, S. Guhan, D. Low, Downstream processing of monoclonal antibodies – application of platform approaches, J. Chromatogr. B Anal. Technol. Biomed Life Sci. 848 (2007) 28–39, https://doi.org/10.1016/j.jchromb.2006.09.026.

[57] M.C. Neves, P. Pereira, A.Q. Pedro, J.C. Martins, T. Trindade, J.A. Queiroz, M. G. Freire, F. Sousa, Improved ionic-liquid-functionalized macroporous supports able to purify nucleic acids in one step, Mater. Today Bio. 8 (2020), 100086, https://doi.org/10.1016/J.MTBIO.2020.100086.